

Electronic supplementary information (ESI)

Full-capped 12-S-atom TTP derivatives (BV-TTP, BE-TTP, EM-TTP and EV-TTP): Syntheses, Structures and charge transport properties

Qi Fang,^{*ab} Hong-feng Chen,^a Hong Lei,^c Gang Xue^a and Xia Chen^a

^a State Key Laboratory of Crystal Materials, Shandong University, 250100 Jinan, P. R. China. Fax: +86 531 88362782; Tel: +86 531 88363497; **E-mail: fangqi@sdu.edu.cn**

^b School of Chemistry and Chemical Engineering, Shandong University, 250100 Jinan, P. R. China.

^c School of Information Science and Engineering, Shandong University, 250100 Jinan, P. R. China

Contents

- ¹H NMR spectra of BE-TTF, **BE-TTP**, **EM-TTP**, **EV-TTP**, **BV-TTP**, and BV-TTF (Fig. 7). S1
Fig. 7a. BE-TTF in CDCl₃/TMS.
Fig. 7b. **BE-TTP** in CS₂, with CDCl₃ /TMS external reference.
Fig. 7c. **EM-TTP** in CS₂, with CDCl₃ /TMS external reference.
Fig. 7d. **EV-TTP** in CS₂, with CDCl₃ /TMS external reference.
Fig. 7e. **BV-TTP** in CS₂, with CDCl₃ /TMS external reference.
Fig. 7f. BE-TTF in CDCl₃ /TMS.
Fig. 7g. TTF in CDCl₃ /TMS.
- A discussion about electronic donating and π -conjugation of the title TTP derivatives. S5
- The photographs of the crystal shapes of *m*-**BV-TTP**, **BE-TTP**, **EM-TTP**, and **EV-TTP** and the discussion about the determination of the conducting direction (Fig. 9). S8
- A structure drawing of TTM-TTP and TTC₄-TTP (based on the CCDC X-ray data) with the electronic transfer integral (*t*) being indicated (Fig. 10). S9
- A photograph of a **EV-TTP** crystal with two gold wires and gold-paste on it for conductivity measurement (Fig. 11) S9
- DTA and TG curves of *m*-**BV-TTP**, **EV-TTP**, **BE-TTP**, and **EM-TTP** (Fig. 12). S10
- A drawing of the improved Soxhlet's extractor (Fig. 13). S11
- IR spectra of *t*-**BV-TTP**, *m*-**BV-TTP**, **BE-TTP**, **EV-TTP**, and **EM-TTP** (Fig. 14). S12

1. ^1H NMR spectra of BE-TTF, BE-TTP, EM-TTP, EV-TTP, BV-TTP, and BV-TTF (Fig. 7).

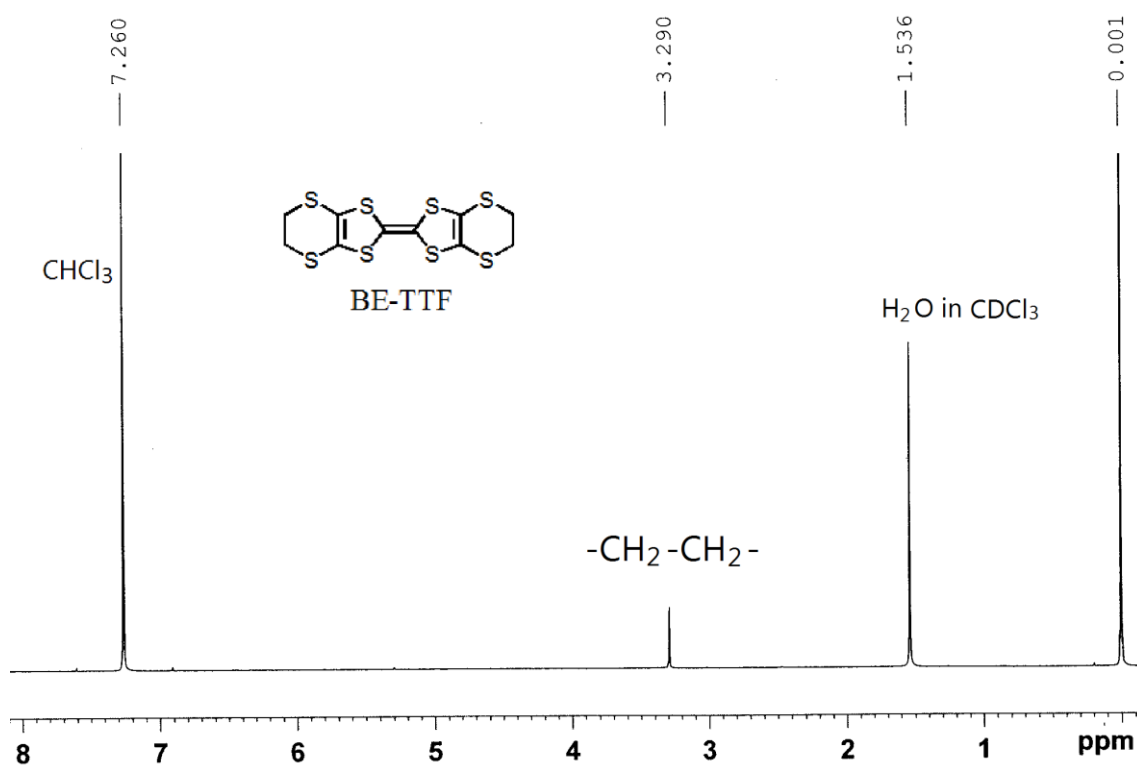


Fig.7a BE-TTF in CDCl_3 /TMS

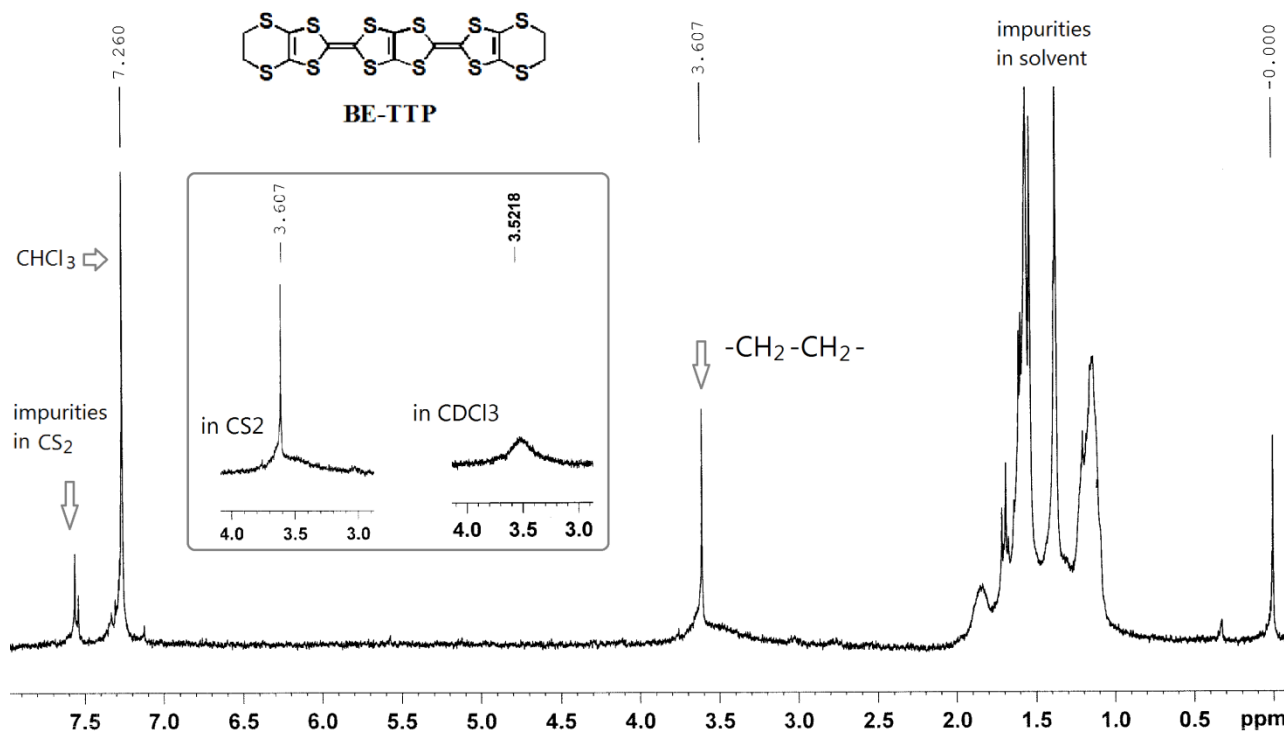


Fig. 7b BE-TTP in CS_2 , with CDCl_3 /TMS external reference. The inset is a comparison of the spectrum from CS_2 solution and that from CDCl_3 solution

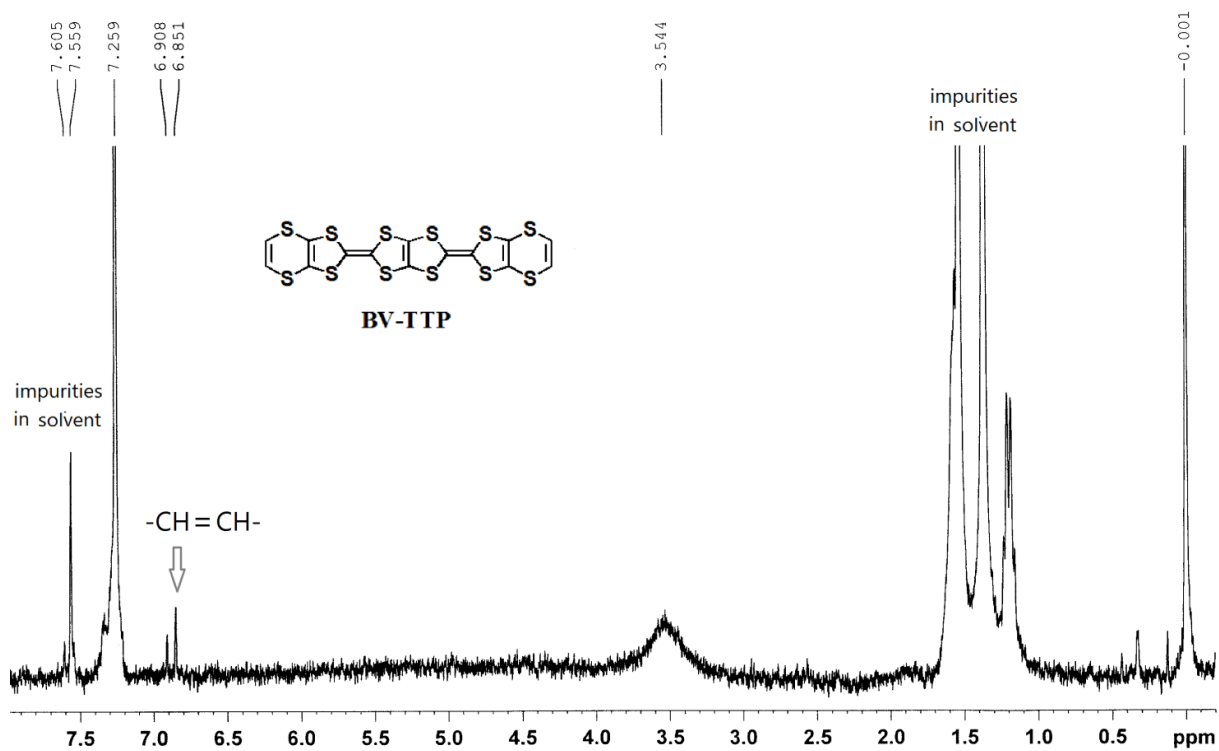


Fig. 7e BV-TTP in CS₂, with CDCl₃/TMS external reference.

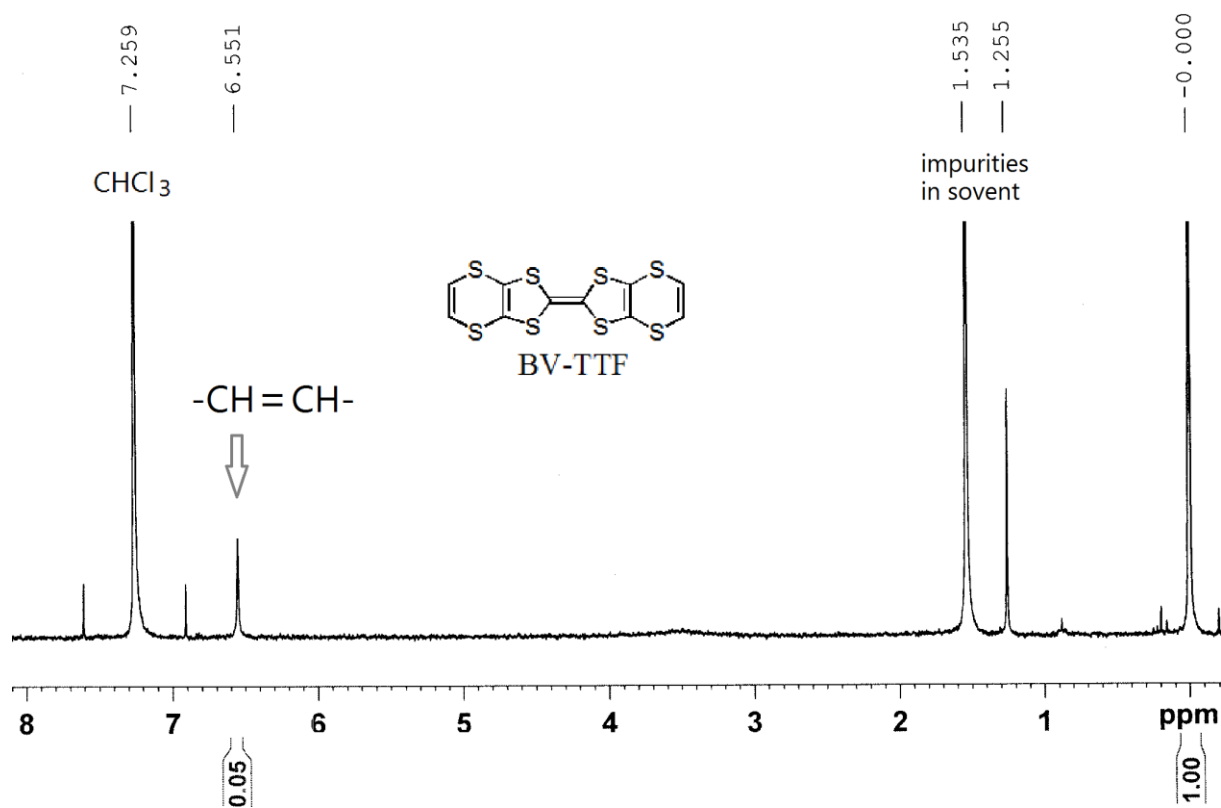


Fig. 7f BV-TTF in CDCl₃/TMS.

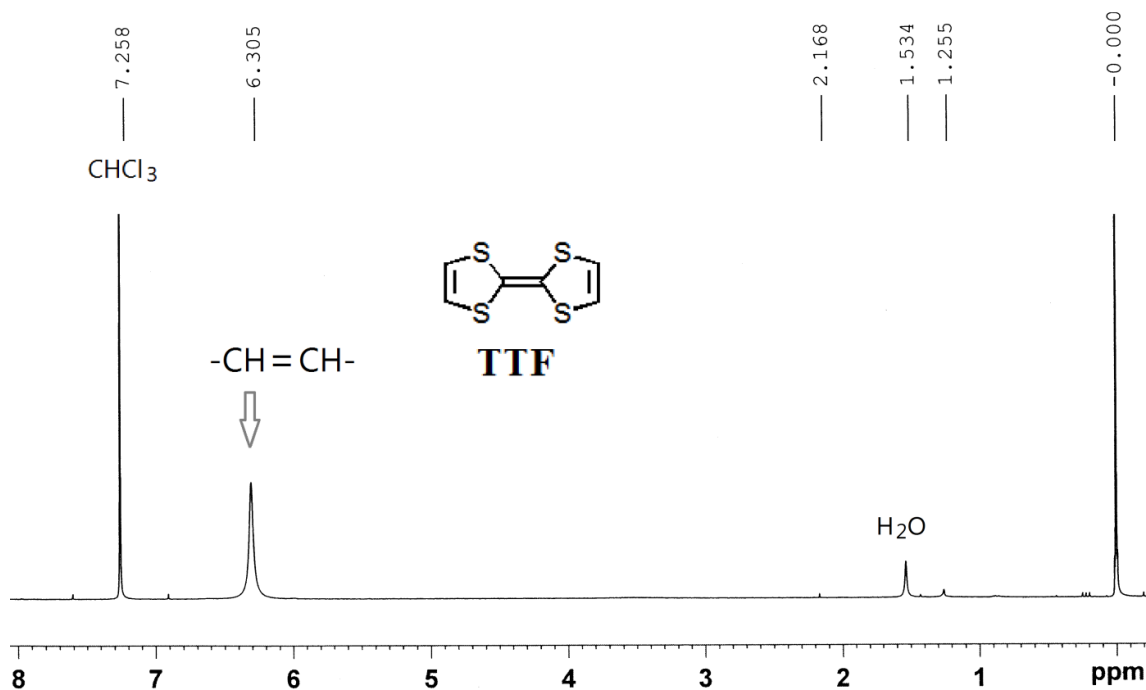


Fig. 7g TTF in CDCl_3/TMS

Fig. 7 ^1H NMR spectra of BE-TTF, **BE-TTP**, **EM-TTP**, **EV-TTP**, **BV-TTP**, BV-TTF, and TTF. Because of the extreme low solubility of the full-capped 12-S-atom TTP derivatives in deuterio reagents, CS_2 had to be used as the solvent. CDCl_3/TMS , which is in a capillary and in the NMR tube, was used as the external references. The spectra of BE-TTF, BV-TTF, and TTF are normally in CDCl_3/TMS .

2. A discussion about electronic donating and π -conjugation of the title TTP derivatives.

2-1 About the electronic donating property

Electronic donating property in this work is investigated in terms of:

- (A) Redox potential measurement, which measure the donating property in solution;
- (B) Ionization potential calculation, which measure the donating property in gas.

For all the 12-S-atom TTP derivatives in Table 4, the sequence of the first redox potentials (E_1) is basically in consistent with the sequence of the calculated first ionization potentials (I_1). The E_1 values of **BE-TTP** and **BV-TTP** are lower than that of BE-TTF and BV-TTF, respectively. This indicates that the electron donating ability has an increase when the TTF-core in 8-S-atom TTF derivatives is replaced by the bis-fused TTF core, yielding the 12-S-atom TTP derivatives.

Table 4 Measured redox potentials and calculated ionization potentials ^a, and absorption positions

	E_1/V	E_2/V	$\Delta E_{12}/V$	I_1/eV	I_2/eV	$\Delta I/12$	λ_{abs}^b experimental	λ_{abs}^c theoretical
BE-TTF	0.66	0.86	0.20	6.105	9.743	3.64	323 nm	305.5 nm
BE-TTP	0.58	0.72	0.14	5.987	8.887	2.90	341 nm	333.3 nm
EM-TTP	0.63	0.76	0.13	6.045	8.962	2.92		334.3 nm
EV-TTP	0.67	0.80	0.13	6.074	9.011	2.94		333.8 nm
BV-TTP	0.68	0.81	0.13	6.174	9.128	2.95		332.1 nm
BV-TTF	0.82	0.98	0.16	6.339	10.035	3.70		286.5 nm

^a Ionization potentials (I_1 and I_2) were calculated by DFT/b3lyp method by Gaussian-03 programs, 6-311 + g* basis set was adopted for the geometry optimizations and the energy calculations

^b The long- λ peak position of the UV-vis absorption spectra, recorded in toluene solvent.

^c The theoretical long- λ peak positions were calculated by TD-DFT/6-31(d) method.

2-2 About the π -conjugation property

π -Conjugation property can be studied by means of:

- (A) UV-vis absorption (experimentally or theoretically);
- (B) Direct structural data (X-ray structure and theoretically optimised geometric structure);
- (C) $\Delta E_{12} = E_2 - E_1$ and $\Delta I = I_2 - I_1$.

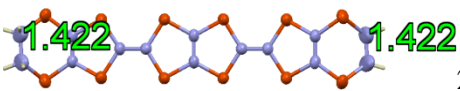
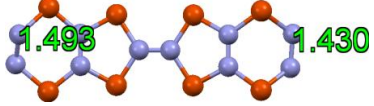
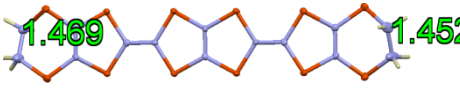
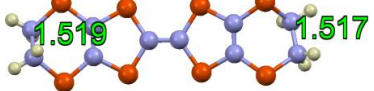
(A) The insolubility of the title TTP compounds make the record of an UV-vis absorption spectrum very difficult. The absorption of CS₂, the only practical solvent, severely overlaps the absorption of our compounds. Fortunately, we found that **BE-TTP** can slightly dissolve in hot toluene and had its UV-vis spectrum recorded (Fig 1b). The red-shift ($\Delta\lambda_{\text{abs}} = 341 - 323 = 18$ nm) of the absorption peaks of **BE-TTP** (relative to BE-TTF, Fig. 1b) indicates its better π -conjugation.

The calculated absorption positions (listed in the last column of Table 4) are consistent with the experimental absorption peak positions

(B) In considering the structural data, we paid an attention to the terminal C-C bond because it is the only kind of bond that connect H atoms, which may make it possible to correlate the bond with the ¹HNMR data.

As we know, the X-ray measured bond lengths are temperature dependent and the DFT optimised bond lengths are basis-set dependent. As listed in Table 5, the terminal C-C bond length of **BE-TTP** is invariably shorter than that of BE-TTF, at high and low experimental temperature and at various basis-set of DFT calculation (from the moderate set of 6-311g(d) to the very large set of 6-311++(3df,3pd)). Thus, we believe that **BE-TTP** has better π -conjugation relative to BE-TTF

Table 5 The terminal C-C bond lengths of **BE-TTP** and BE-TTF

	BE-TTP		BE-TTF	
X-ray diffraction		294K		295K Bull.Chem.Soc.Jpn.,1986, 59, 301. CCDC: CIMZON10
		90K		100 K Acta cryst. C, 2002,56, 453. CCDC: CIMZON03
	Bond length/Å	Basis set	Bond length/Å	Basis set
Results of DFT optimization	1.51750	6-311g(d)	1.51759	6-311g(d)
	1.51745	6-311+g(d)	1.51755	6-311+g(d)
	1.51803	6-311++(3df,3pd)	1.51828	6-311++(3df,3pd)

(C) As revealed in Tables 4, the $\Delta E_{12} = E_2 - E_1$ and $\Delta I_{12} = I_2 - I_1$ values monotonically decrease with increasing the π -dimension from BE-TTF to **BE-TTP**, and from BV-TTF to **BV-TTP**. Therefore the ΔE_{12} or, more conveniently, the ΔI may be a measure for degree of π -conjugation in a series of π -functional compounds. Fig. 8 shows an example of ΔI and π -dimension correlation.

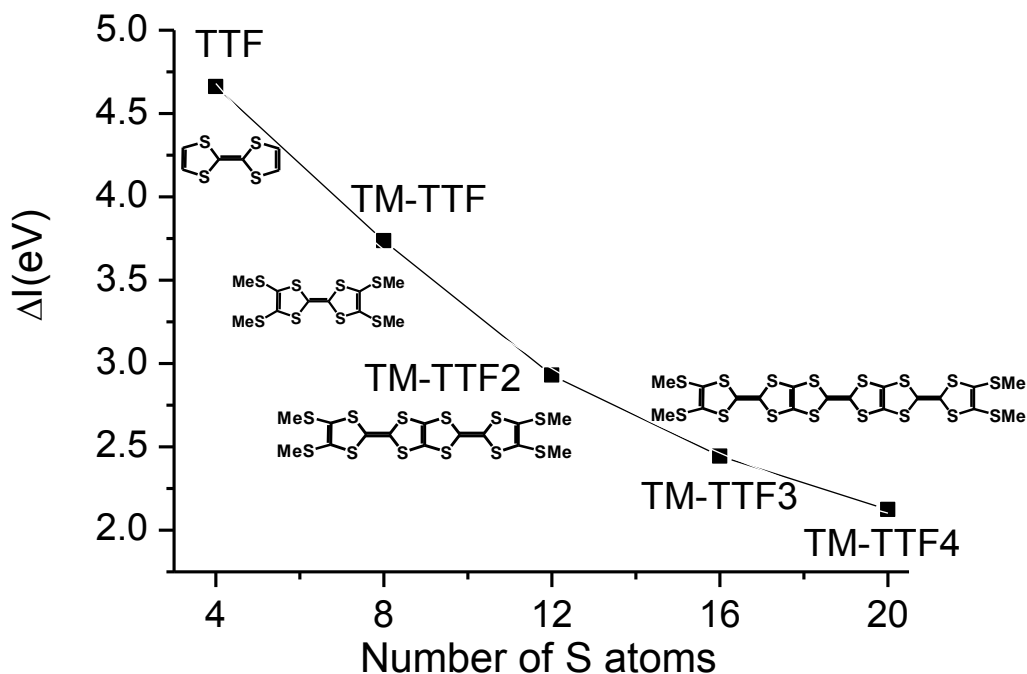


Fig. 8 The ΔI and π -dimension relation for a series of TTF derivatives. TTF2 means the bis-fused TTF core, TTF3 the tris-fused TTF core, TTF4 the tetra-fused core. The calculations were carried out by the DFT/b3lyp method by using Gaussian-03 programs. the 6-311+g* bases were adopted for the geometry optimizations and the energy calculations for all the neutral molecules M, the radical cations M^+ , and the dications M^{2+} .

3. The photographs of the crystal shapes of *m*-BV-TTP, BE-TTP, EM-TTP, and EV-TTP and the discussion about the determination of the conducting direction.

Generally, our crystals are long-bar-shaped or long-plate-shaped, which are well developed along a direction to form the long-axis of the crystal. The conductivity was measured along this direction of the long-axis. To know the direction of conductivity is to know the crystallographic direction $[uvw]$ of this long-axis.

By using a Bruker APEX II diffractometer and the APEX program, we can determine the Miller indexes (hkl) of all the actual faces of the crystal. Then by using the Zone Law, the zone axis $[uvw]$ can be determined which is just the direction of the long-axis of the crystal.

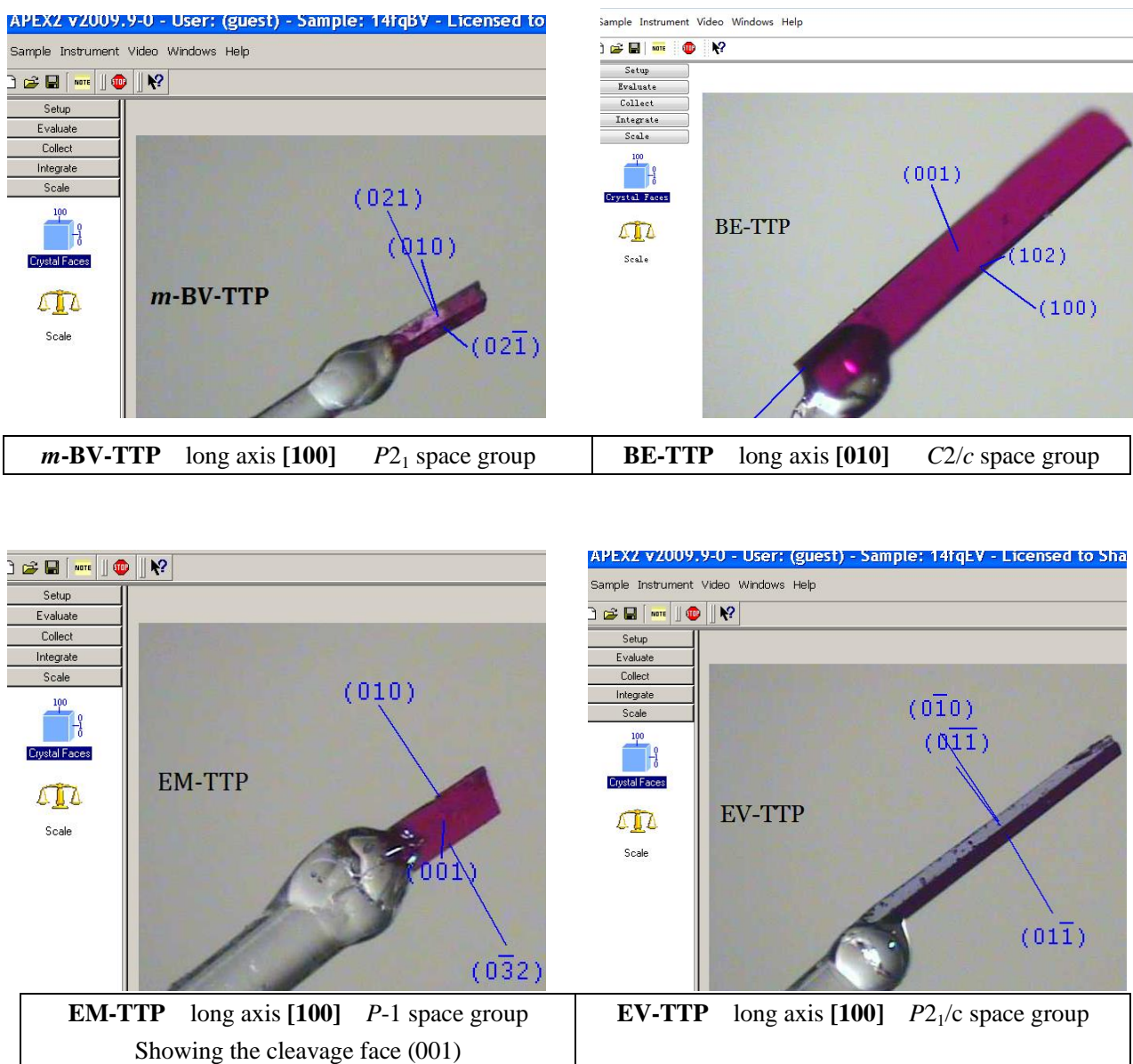


Fig. 9 The photographs of the crystal shapes of *m*-BV-TTP, BE-TTP, EM-TTP, and EV-TTP.

4. A structure drawing of TTM-TTP and TTC_4 -TTP (based on the CCDC X-ray data) with the electronic transfer integral (t) being indicated.

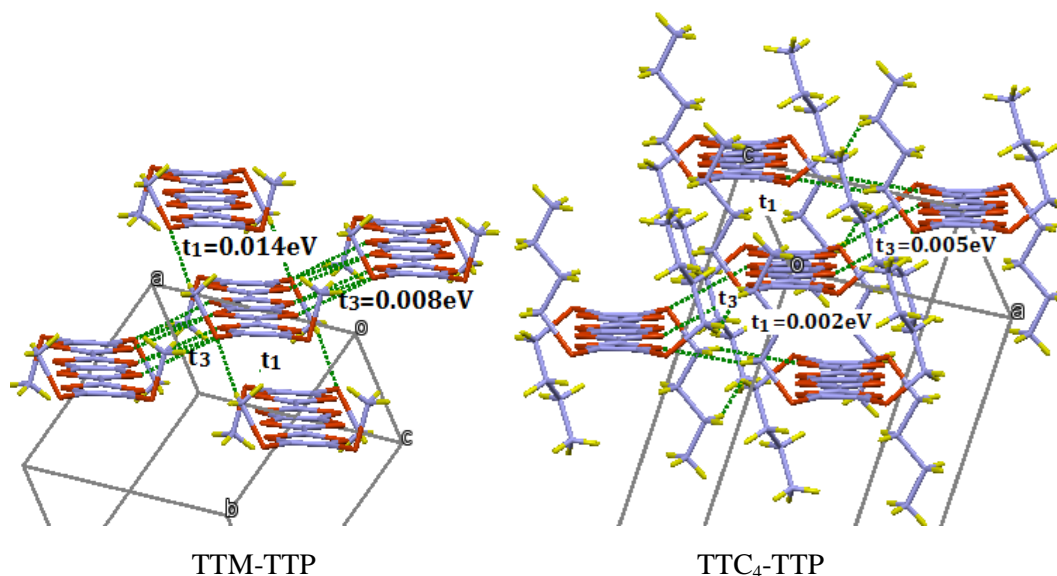


Fig. 10 A structure drawing of TTM-TTP (CCDC No. YATYEX) and TTC_4 -TTP (CCDC No. MEZWUJ) with the electronic transfer integral (t) being indicated. The long terminal alkyl groups make the molecules shift to each other along the short molecular axis and therefore depart from normal face-to-face overlap, which will greatly reduce the columnar π - π interactions.

5. A photograph of a **EV-TTP** crystal with two gold wires and gold-paste on it for conductivity measurement.

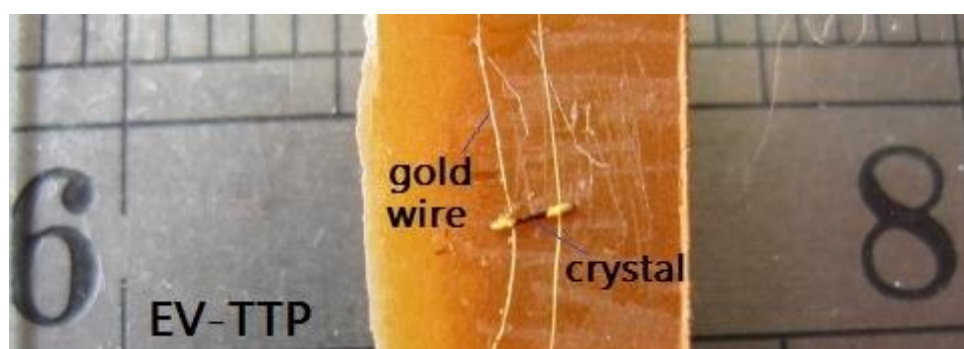


Fig. 11 A photograph of a **EV-TTP** crystal for conductivity measurement. Two gold wires, 0.03 mm in diameter and 1.2 mm apart from each other, were run perpendicularly across the long-bar crystal of **EV-TTP** with dimensions of $1.8 \times 0.08 \times 0.04$ mm and fixed in place using gold-paste.

6. DTA and TG curves of *m*-BV-TTP, EV-TTP, BE-TTP, and EM-TTP

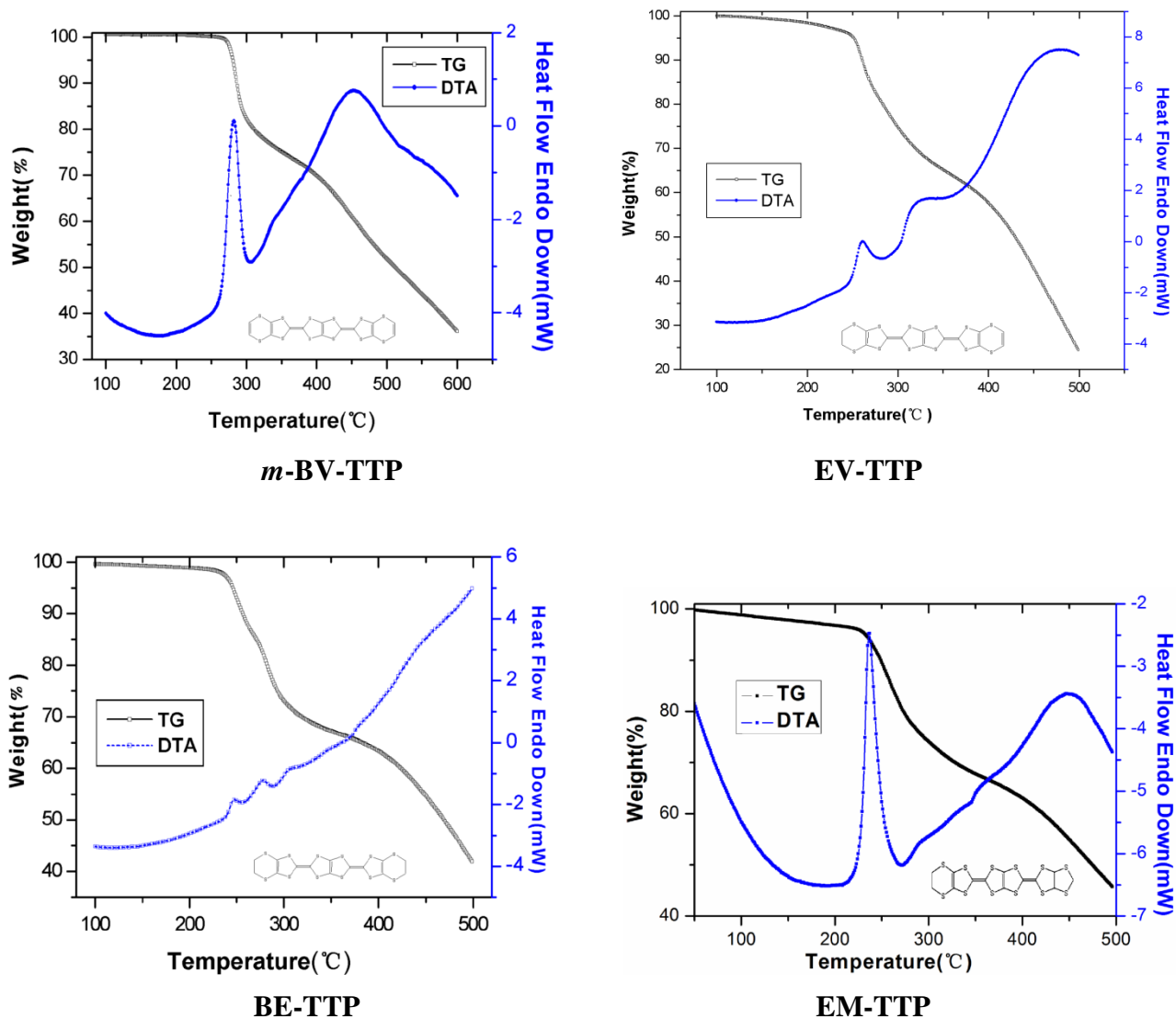


Fig. 12 DTA and TG curves of *m*-BV-TTP, EV-TTP, BE-TTP, and EM-TTP

7. A drawing of the improved Soxhlet's extractor.

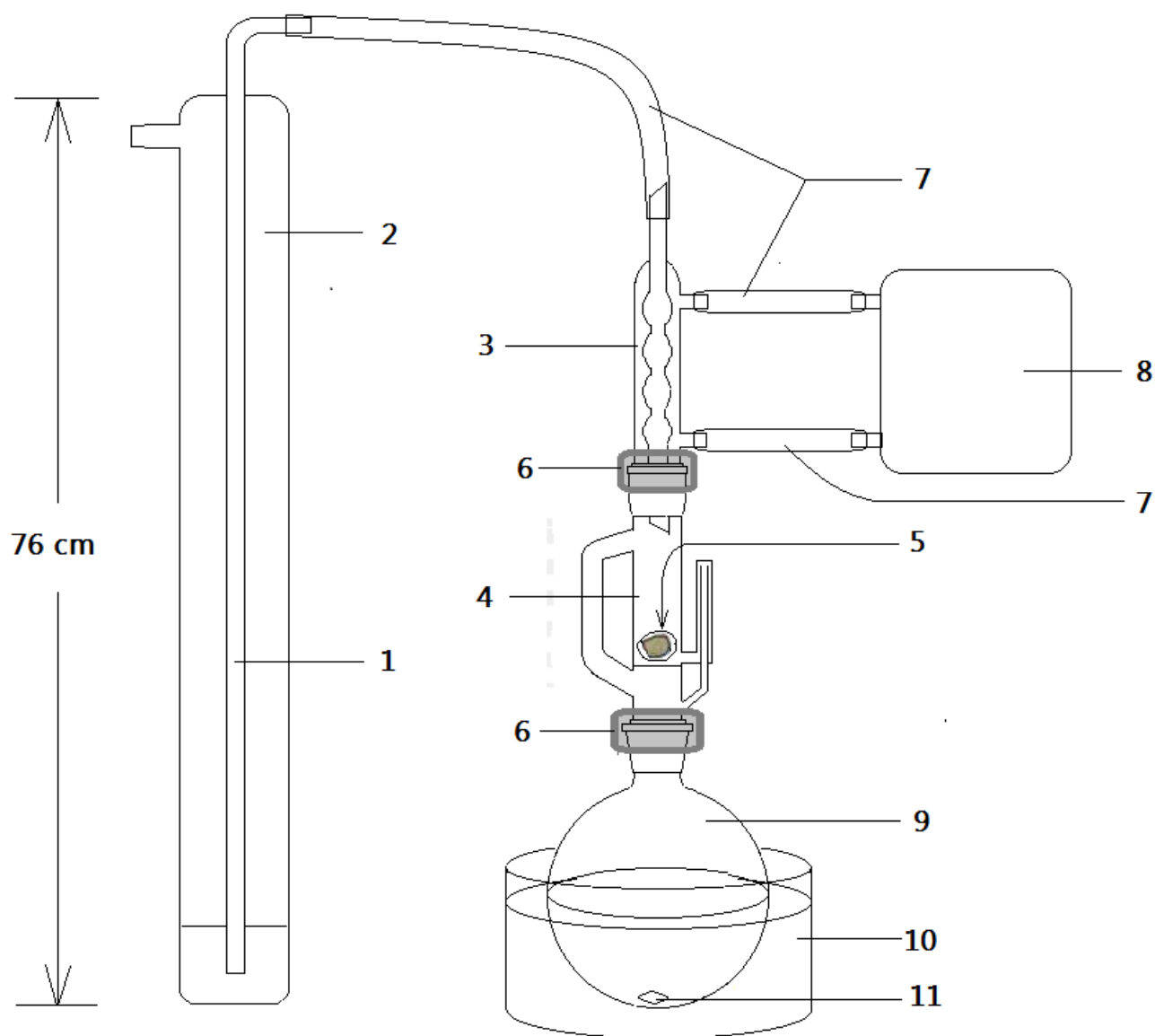
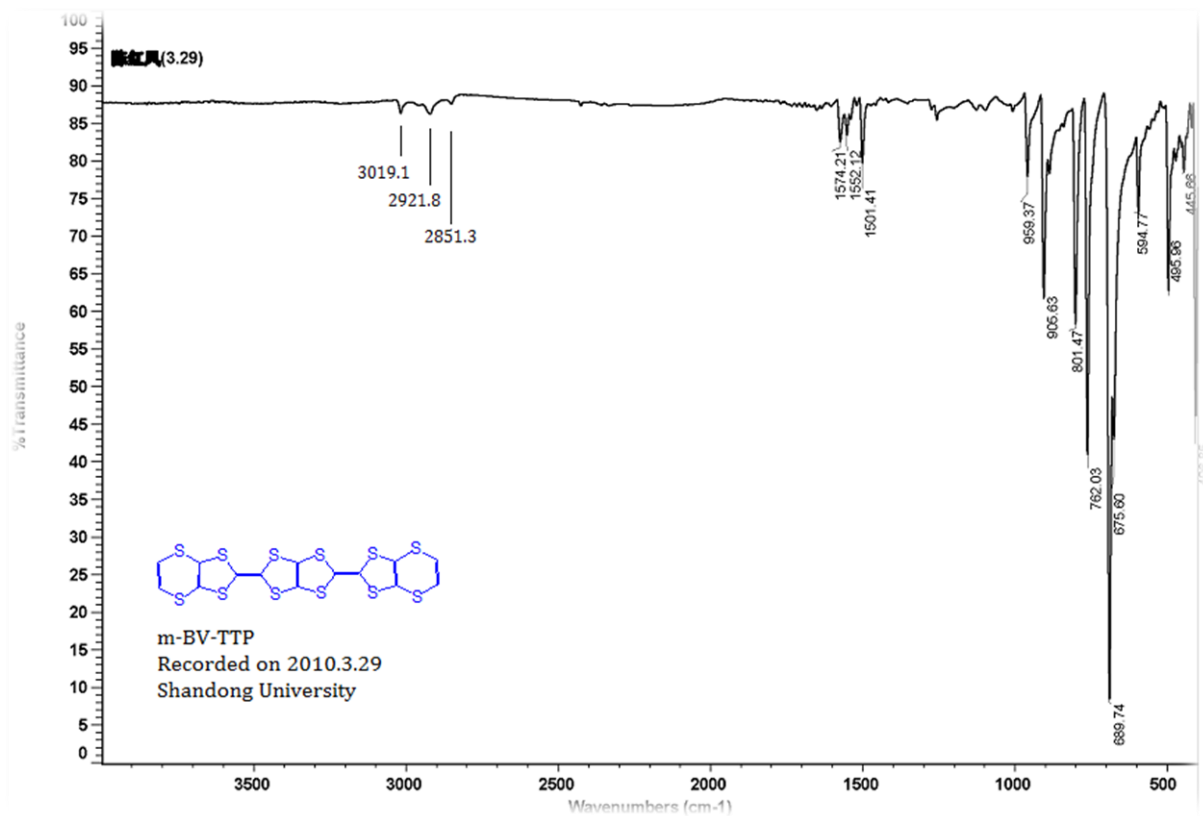
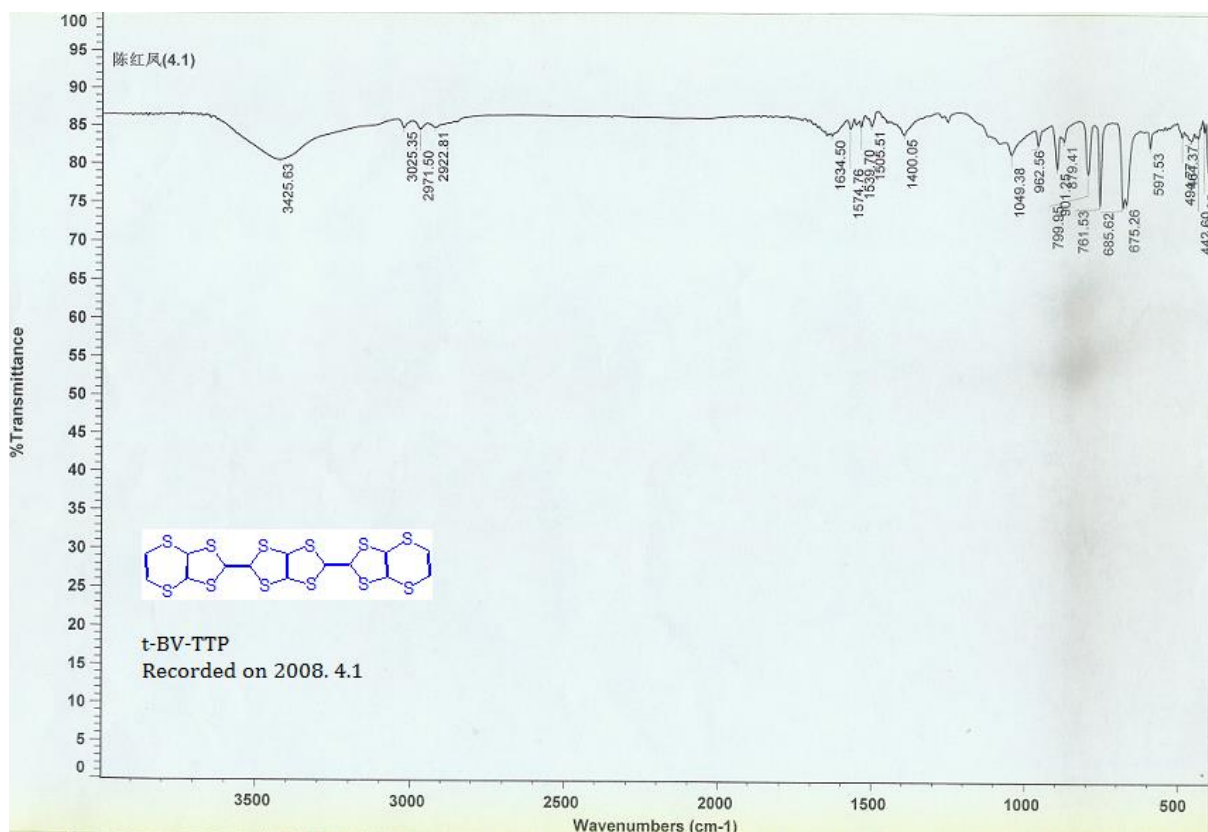
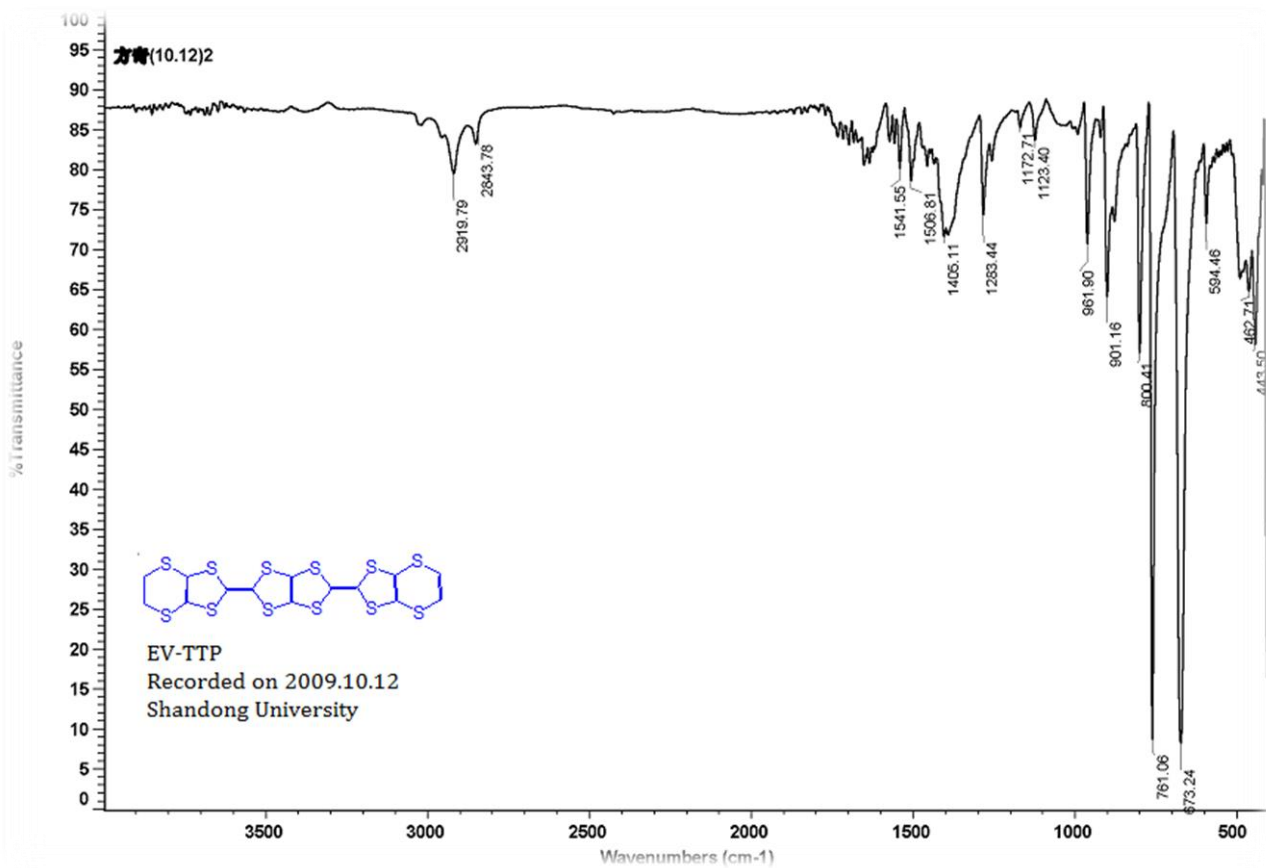
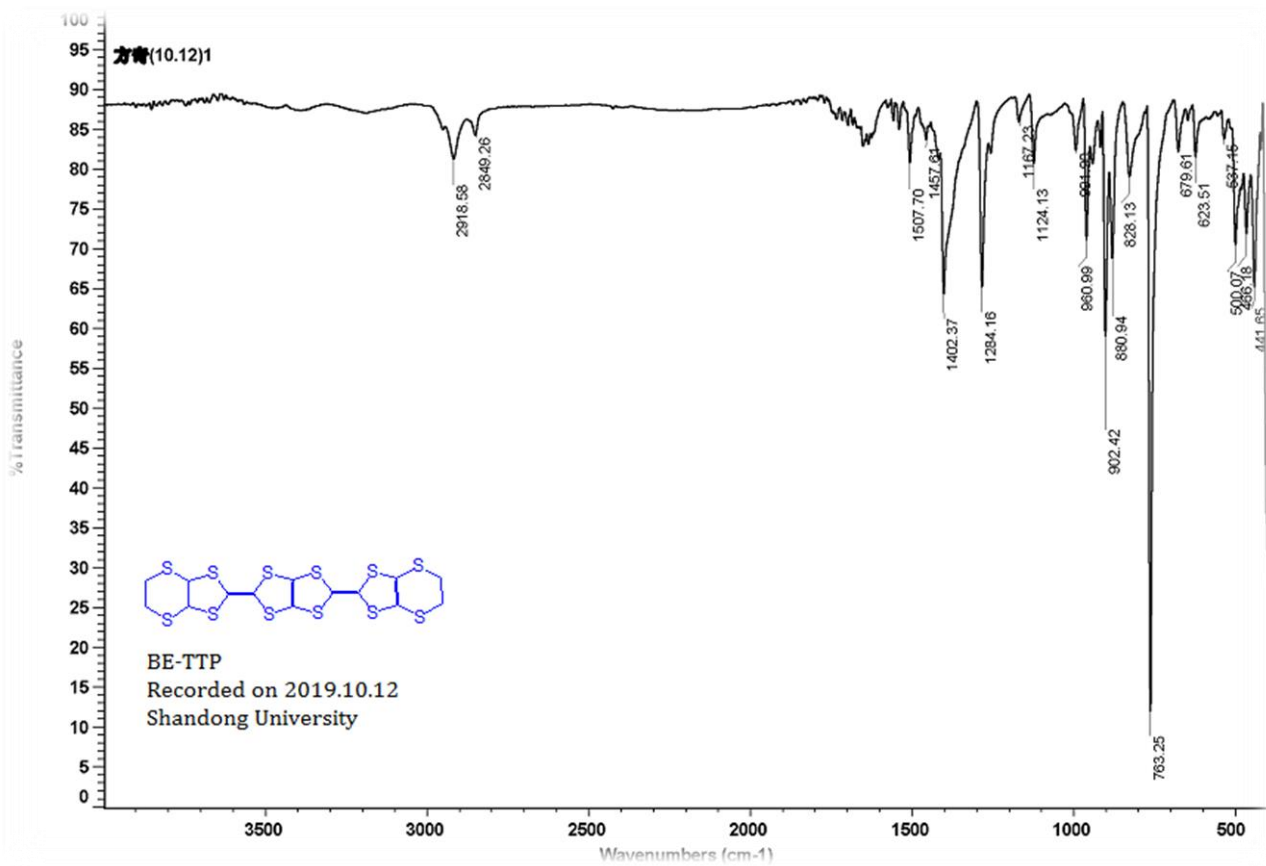


Fig. 13 A improved Soxhlet's extractor.

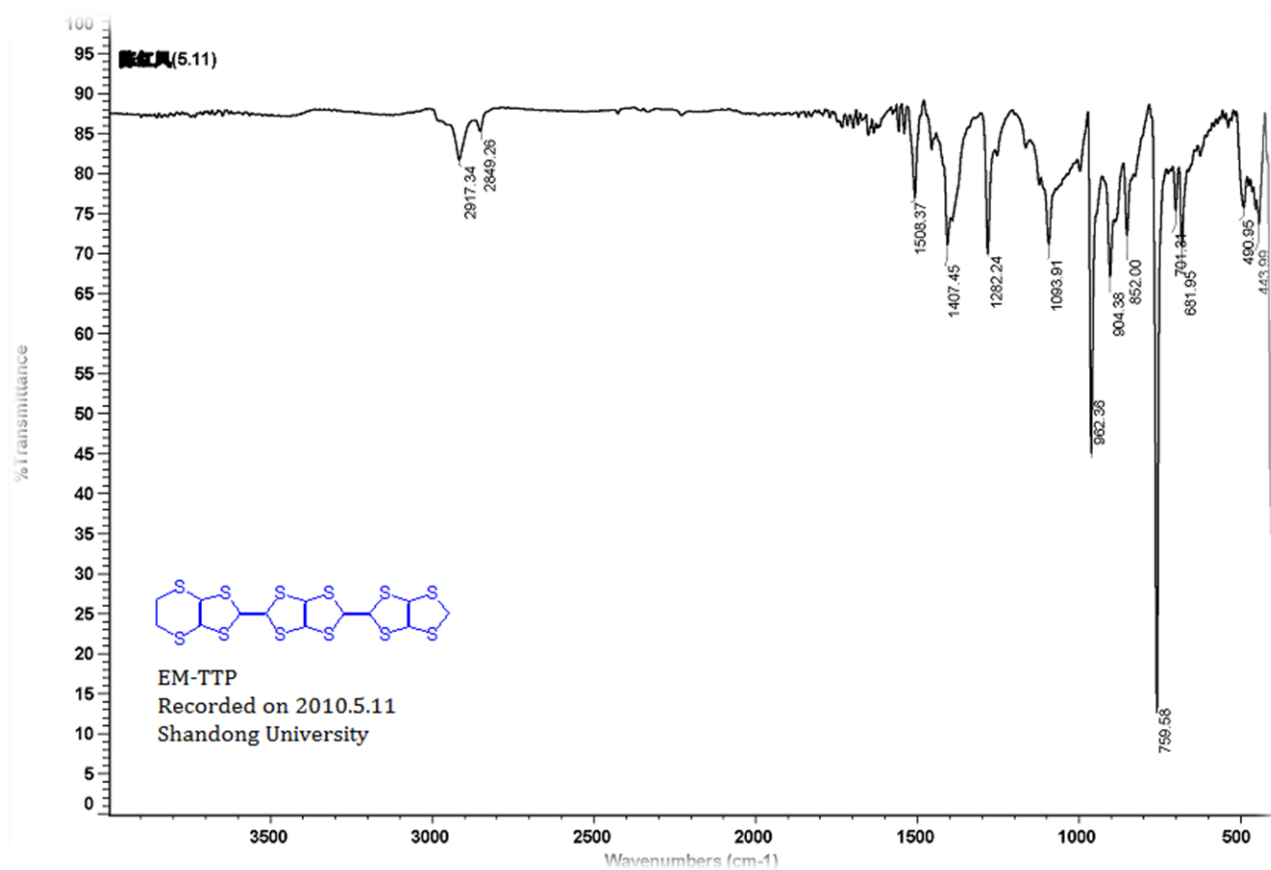
1 and 2: Mercury bubbler; 3: Condenser; 4: Chamber for solid sample; 5: Solid sample in filter paper; 6: Parafilm; 7: Silicone soft tube; 8: Low-temperature cooling liquid circulating pump; 9: Flask; 10: Silicone oil heating bath; 11: Stirrer. The more details can be found in a PRC Patent of the same authors.

8. IR spectra of *t*-BV-TTP, *m*-BV-TTP, BE-TTP, EV-TTP, and EM-TTP





IR spectra of EV-TTP



IR spectra of EM-TTP

Fig. 14 IR spectra of *t*-BV-TTP, *m*-BV-TTP, BE-TTP, EV-TTP and EM-TTP

The triclinic *t*-BV-TTP and monoclinic *m*-BV-TTP can be identified by checking a CH peak, which is at 2972 cm⁻¹ for *t*-BV-TTP and 2922 cm⁻¹ for *m*-BV-TTP. The IR spectrum of EV-TTP is similar to the spectral overlap of BE-TTP and *m*-BV-TTP. Its 1283m and 673s sharp peaks, for example, are corresponding to the character peaks of BE-TTP (1284s) and *m*-BV-TTP (676s), respectively.